International Journal of Nanomedicine

Dovepress
open access to scientific and medical research

Open Access Full Text Article

ORIGINAL RESEARCH

A nanoparticulate injectable hydrogel as a tissue engineering scaffold for multiple growth factor delivery for bone regeneration

This article was published in the following Dove Press journal:
International Journal of Nanomedicine
27 December 2012
Number of times this article has been viewed

Deepti Dyondi[1]
Thomas J Webster[2]
Rinti Banerjee[1]

[1]Department of Biosciences and Bioengineering, Indian Institute of Technology Bombay, Mumbai, Maharashtra, India; [2]Nanomedicine Laboratories, Division of Engineering and Department of Orthopedics, Brown University, Providence, RI, USA

Abstract: Gellan xanthan gels have been shown to be excellent carriers for growth factors and as matrices for several tissue engineering applications. Gellan xanthan gels along with chitosan nanoparticles of 297 ± 61 nm diameter, basic fibroblast growth factor (bFGF), and bone morphogenetic protein 7 (BMP7) were employed in a dual growth factor delivery system to promote the differentiation of human fetal osteoblasts. An injectable system with ionic and temperature gelation was optimized and characterized. The nanoparticle loaded gels showed significantly improved cell proliferation and differentiation due to the sustained release of growth factors. A differentiation marker study was conducted, analyzed, and compared to understand the effect of single vs dual growth factors and free vs encapsulated growth factors. Dual growth factor loaded gels showed a higher alkaline phosphatase and calcium deposition compared to single growth factor loaded gels. The results suggest that encapsulation and stabilization of growth factors within nanoparticles and gels are promising for bone regeneration. Gellan xanthan gels also showed antibacterial effects against *Pseudomonas aeruginosa*, *Staphylococcus aureus*, and *Staphylococcus epidermidis*, the common pathogens in implant failure.

Keywords: bone tissue engineering, bone morphogenetic protein 7 (BMP7), basic fibroblast growth factor (bFGF), hydrogel, nanoparticles, osteoblasts

Introduction

Current methods for bone restoration (such as autografts, allografts, and bone cement) offer several complications, such as insufficient osseointegration, undesirable tissue responses, and increased risk of infection at the implant site, all of which may lead to implant failure.[1,2] Such limitations of current bone restoration methods and materials warrant a new set of biomaterials.

Bone tissue engineering has emerged as a promising alternative with an ability to deliver osteoconductive as well as osteoinductive (such as growth factors and cytokines) materials to the defect site.[3] Bone tissue engineering, which uses biodegradable polymers (such as hydrogels), allow for a great deal of flexibility with respect to their tunable mechanical properties and natural degradation times within the body. Apart from tailoring polymer functional groups for promoting cell material interactions, the polymer can also be tailored to gel and harden in situ for developing minimally invasive bone regeneration procedures. A wide choice of molecules may be delivered to the bone defect site for regional effects, like growth factors, drug molecules, and recombinant proteins.[4,5]

Most importantly, hydrogels initially developed for soft tissue engineering applications are now being explored for bone regeneration by incorporating

Correspondence: Rinti Banerjee
Department of Biosciences and Bioengineering, Indian Institute of Technology Bombay, Mumbai, Powai, Maharashtra 400076, India
Tel +91 22 2576 7868
Fax +91 22 2572 3480
Email rinti@iitb.ac.in

hydroxyapatite and other phases of Ca-P (the main inorganic component of bone). The current study explores natural polymers, namely gellan and xanthan, for developing a nanoparticulate in situ gelling system which along with cells and growth factors may be delivered at the defect site. Gellan gum, an anionic exocellular polysaccharide derived from the bacteria *Sphingomonas elodea*, is composed of repeating tetrasaccharide units consisting of glucose, glucuronic acid, and rhamnose residues in a 2:1:1 ratio joined in a linear chain. With a melting and setting point ranging from 30°C–50°C, this polysaccharide offers excellent gel stability and flexibility.[6] Xanthan gum is an anionic exocellular polysaccharide produced from the bacteria *Xanthmonas campestris*. It has a β-1, 4-linked D-glucose backbone, and therefore, is identical to the cellulose molecule. Solutions of xanthan are known to be pseudo plastic; stable to variations in pH, temperature, and salt concentrations; show a rapid regain of viscosity upon removal of shear stress; and show optimal suspension properties and high viscosity at low shear rates.[7]

The versatility of gellan to be used as scaffolds, fibers, particles, or membranes as well as its ability to support human nasal chondrocytes growth and proliferation has been shown in studies by Oliveira et al.[8,9] Studies with human and rat articular chondrocytes have also proven its potential as a promising material for cartilage tissue regeneration.[9,10] A gellan xanthan combination has been shown to be a promising injectable gel system that could act as a supporting matrix for cells to regenerate cartilage, by our group.[11] With an excellent water holding capacity and hydrophilicity, gellan xanthan gels show a gelling time of <10 minutes at room temperature and <5 minutes at 37°C which make them suitable for the intended application.[11] The hydrogel was optimized such that it allowed for modification/addition of growth factors and cells while it still was in a liquid state at room temperature and could gel once placed inside the defect site. The current study involved evaluating this polymer combination as a potential injectable matrix for supporting bone regeneration along with the growth factors basic fibroblast growth factor (bFGF) and bone morphogenetic protein 7 (BMP7).

Growth factors, owing to their short half-life, are cleared quickly from the defect site; therefore, encapsulating these growth factors within nanocarriers is advantageous over direct injections. Growth factors also show minimal tissue penetration which may lead to inefficient delivery at the defect site. Chitosan nanoparticles were developed here and characterized for the delivery of the growth factors. Nanoparticles, being small in size, allow for easy penetration and a better control over dosage and the delivery period of biomolecules thereby enhancing the in vivo efficacy of the growth factors which is crucial for tissue regeneration.[12] Out of the 20 different BMPs known, BMP7 (osteogenic protein, OP1) and BMP2 have demonstrated bone formation and fracture healing properties in several in vivo studies leading to their approval for clinical testings.[13–16] BMP7, also belonging to the transforming growth factor beta (TGF-β) superfamily of proteins, is known to stimulate proliferation of bone cells and alkaline phosphatase production, mediated by increased production of insulin-like growth factor.[17,18] bFGF has an angiogenic effect, allows proliferation of osteoblast cells, and thus accelerates bone regeneration.[19,20] bFGF loaded gelatin hydrogels implanted in rabbit cranial defects showed an enhanced bone mineral density in skull defects as observed by hematoxylin and eosin staining.[21] Furthermore, the materials employed for tissue engineering were also evaluated for antimicrobial properties in an attempt to study the effectiveness of the injected material to resist bacterial growth at the implanted site, thereby resisting implant failure. Antimicrobial coatings based on drug elution techniques have demonstrated only short-term antimicrobial effects, often presenting the risk of toxicity or developing microbe resistance.[22] An implant material that exhibits anti-bacterial effects by itself is desirable. Chitosan nanoparticles (growth factor carrier) were used along with gellan xanthan gels to develop an in situ gelling biomaterial combining the viscoelasticity of natural polymers with the powerful antimicrobial properties of chitosan. The components of the injectable system were tested for antibacterial efficacy against *Pseudomonas aeruginosa*, *Staphylococcus epidermidis*, and *Staphylococcus aureus*; multiple antibiotic resistant strains of bacteria clinically prevalent in orthopedic implant infections.[23] The current study aimed at developing a contamination-free injectable scaffold system for dual growth factor delivery in bone regeneration.

Materials and methods

Materials

Gellan gum and xanthan gum were purchased from Spectrum Chemicals (Gardena, CA) which was evaluated as an in situ gelling system. Chitosan was bought from Marine Chemicals (Kerala, India). Pentasodium tripolyphosphate (TPP) was purchased from CDH Laboratories (New Delhi, India). A Milli-Q water system (Millipore, Bedford, MA) provided high purity water (18.2 MΩ · cm) for all experiments.

Dulbecco's modified Eagle's medium (DMEM), antibiotic antimycotic solution, and fetal bovine serum (FBS) were purchased from Sigma-Aldrich (St Louis, MO).

Minisart 25 mm, 0.2 microns syringe filters were purchased from Sartorius (Göttingen, Germany). Easyflask 25 filt NUNCLON tissue culture flasks were purchased from NUNC (Penfield, NY). Growth factors BMP7 and bFGF were purchased from R&D Systems (Minneapolis, MN). Enzyme-linked immunosorbent assay (ELISA) kits were bought from Ray Biotech (Norcross, GA).

Hydrogel preparation and characterization

Gellan xanthan gels

The polymers [gellan and xanthan (in a 9:1 gellan:xanthan ratio)] were used for hydrogel preparation; 0.9% gellan:xanthan (9:1) with 3 mM Ca (GX3) had been developed and characterized in earlier studies by the group.[11] For the current study, Ca^{+2} ions were replaced by DMEM as the source of cations for gelation. Briefly, DMEM media was heated to 80°C–90°C and the polymer mixture was added slowly, with continuous stirring, for complete dissolution in the media. The gelation process was initiated as the solution was allowed to cool down. The gel was characterized for flow behavior/viscosity and viscoelasticity.

Rheological measurements and scanning electron microscopy (SEM)

Rheological measurements were performed using a MCR301 RHEOPLUS/32 (Anton Paar, Graz, Austria) rheometer (CC27 measuring system, cup and bob). Frequency (0.1–100 Hz) and amplitude (0.09–50 strain %) sweeps were done for 0.9%, 0.7%, and 0.5% 9:1 gellan xanthan gels in DMEM (solid) at 37°C. The samples were also tested for viscosity at a constant shear rate of 0.5/second. Further viscosity vs temperature and viscosity vs shear stress profiles for all three concentrations of gellan xanthan gels were also evaluated. Viscoelasticity was quantified in terms of G′ (storage modulus) and G″ (loss modulus), the real and imaginary components of the complex shear modulus of the material respectively.

The hydrogel microstructure was observed under SEM (Hitachi S-3400N; Hitachi Ltd, Tokyo, Japan). Lyophilized gels were gold sputtered and visualized at an accelerating voltage of 10 kV.

Carrier characterization and anti-bacterial study

Chitosan nanoparticle preparation and characterization

Chitosan nanoparticles were prepared by the ionic gelation method. Briefly, an aqueous solution of TPP (0.1%–0.2% w/v) was added to a chitosan aqueous solution (0.1%–0.2% w/v in 0.25% v/v acetic acid) under magnetic stirring at room temperature, until the appearance of slight turbidity.[24] The particles, thus formed, were centrifuged at 9000 g for 30 minutes. The supernatant was discarded and the pellets obtained were resuspended in distilled deionized water. Particle characterization was completed by dynamic light scattering (Brookhaven Instruments Corporation, Holtsville, NY). Particle size, morphology, and particle distribution were examined using a transmission electron microscope (TEM; model CM200; Philips, Amsterdam, Netherlands) operating at 120 kV as per the negative staining protocol. For atomic force microscopy (AFM), a drop of nanoparticles was dropped onto a coverslip and air dried. The sample was analyzed as is in the tapping mode of AFM Veeco Dimensions 3100 SPM with Nanoscope IV controller instrument (Veeco Instruments Inc, Plainview, New York, USA). Image analysis for surface roughness and particle size was done using Nanoscope Image Analysis software (Veeco Instruments Inc) in an offline mode.

Protein loading and in vitro release

BMP7 was loaded onto chitosan nanoparticles by rehydrating 1 mg of lyophilized nanoparticles with 100 µL protein in 1 mL phosphate buffered saline (PBS; 1 µg/mL BMP7 concentration) overnight. After the rehydration process, the unencapsulated growth factor was collected by centrifuging the protein-nanoparticle suspension at 1500 rpm for 10 minutes. The supernatant was assayed for unencapsulated growth factor by a ELISA BMP7 kit. For monitoring the release kinetics, 1 µg/mL BMP7 was loaded in chitosan nanoparticles entrapped within gellan xanthan gel and release was performed in 15 mL of PBS (pH 7.4) at 37°C in a shaking water bath at 150 rpm. The release media contained PBS, 2 mM sodium azide, and 0.01% BSA; 1 mL samples were withdrawn at prefixed time intervals and replaced by the same volume of PBS. The amount of BMP released was determined by a BMP7 ELISA kit. 100 µL of BMP7 was entrapped in the hydrogel (0.33 ng of growth factor) and release was carried out in 10 mL of PBS, pH 7.4 at 37°C in a shaking water bath at 150 rpm. One microliter mL aliquots were withdrawn at different time intervals for 21 days and frozen at −80°C for further quantification. The release was carried out in triplicate and quantification was completed using an ELISA kit following the assay procedures.

Anti-bacterial activity: crystal violet staining

Anti-bacterial activity of the hydrogel components was evaluated to test the possible risk of infection due to the hydrogel components at the injection site. Three strains

of bacteria (known to cause inflammation, pus formation, and tissue necrosis): *S. epidermidis*, *P. aeruginosa*, and *S. aureus* (American Type Culture Collection: 35984, 25668, and 25923, respectively) were used for the study. These strains have been well known to cause implant associated infection.[23,25,26] Bacterial suspensions were obtained by protocols described previously.[26,27] Two hundred microliters of the bacterial suspension was added to each of the wells containing the material to be tested (chitosan nanoparticles and gellan xanthan gels). After 12 and 24 hours, the wells were rinsed with 1X PBS twice. 125 µL of crystal violet stain was added to each well and kept for 15 minutes at room temperature (25°C). The wells were then rinsed again with PBS and the plates were allowed to dry overnight. One hundred microliters of 100% ethanol was added to each well plate and the absorbance was read at 562 nm.

Osteoblast culture

Human fetal osteoblasts (bone-forming cells; CRL-11372 American Type Culture Collection) were cultured in HyClone DMEM (Thermo-Fisher Scientific, Waltham, MA)/F-12 Ham media supplemented with 10% FBS (Hyclone) and 1% penicillin/streptomycin (P/S; Hyclone) under standard cell culture conditions (that is, a sterile, 37°C, humidified, 5% CO_2/95% air environment). Cells at population numbers 2–4 were used in the experiments without further characterization.

In vitro cell viability: L929 mouse fibroblasts and human fetal osteoblasts

MTT assay

The in vitro toxicity of the polymers was measured using L929 mouse fibroblast cells (National Centre for Cell Sciences, Pune, India) as well as human fetal osteoblasts and a MTT (3-(4,4-dimethylthiazol-2-yl)-2,5-diphenyl tetrazolium bromide) assay. Briefly, 1×10^4 L929 cells/well were seeded over disc-shaped gel samples placed in a 24-well plate. The MTT assay for cell viability was completed on day 2 to check for the percentage of viable cells.[28] A similar protocol was followed for the osteoblasts using 50,000 cells per well. The MTT assay was performed after 48 hours for the osteoblasts and was expressed as the percentage of viable cells.

Cell viability: confocal microscopy

At the end of the 48-hour time period, cells were fixed with 10% buffered neutral formalin (Thermo-Fisher Scientific, Waltham, MA) and stained with 4′,6-diamidino-2-phenylindole (DAPI, ex/em ~350 nm/~470 nm) and rhodamine phalloidin (Life Technologies, Carlsbad, CA; ex/em ~550 nm/~580 nm); the cell nuclei and actin filaments of the cells were thus visualized under a confocal microscope (Zeiss LSM510 Meta Confocal Laser Scanning Microscope with an Axiovert 200M inverted microscope; Carl Zeiss AG, Oberkochen, Germany).

A live/dead assay was carried out for cells encapsulated within hydrogels using calcein AM (2 µM) and ethidium homodimer (4 µM) and visualized under a confocal microscope at 10×.

Osteoblast differentiation

For the osteoblast differentiation study, growth factors BMP7 (200 ng/mL) and bFGF (250 ng/mL) were used for evaluating their combinatorial effects on the cells. Briefly, gellan xanthan gels were prepared as described above. At around 40°C, osteoblasts and growth factor loaded nanoparticles were added to the gel formulation and allowed to set. Gel pieces were punched out using a biopsy punch (6 mm diameter) and weighed. Gel constructs containing 10^6 cells/construct and growth factors were put in the wells of a 24-well plate and the cells were cultured in DMEM supplemented with 10% FBS, 1% P/S, 50 µg/mL L-ascorbic acid (Sigma-Aldrich), and 10 mM b-glycerophosphate (Sigma-Aldrich) under standard cell culture conditions for 28 days. The medium was changed every 2 days for all groups. At the end of each time period, samples were freeze dried for 48 hours (LABCONCO FreeZone 6 Liter Freeze Dry System; Labconco, Kansas City, MO) and kept at –20°C until analysis. Cells were lysed to determine total protein content, total collagen content, and alkaline phosphatase activity via well-established commercially available kits (as described later). Calcium deposited by osteoblasts was dissolved in 0.6 mol/L hydrochloric acid and tested for calcium concentration using a commercially available kit.[29]

Papain digestion

Lyophilized hydrogel samples were digested with a papain enzyme solution (10 mM EDTA, 100 mM phosphate, 10 mM cysteine, 125 µg/mL papain enzyme from papaya latex, pH 6.3) at 60°C for 16 hours in a water bath. The papain digested lysate was then evaluated for total DNA, total protein, and glycosaminoglycan content as described below.

Total protein content

Total protein content in the cell lysates was determined using a commercial BCA Total Protein Assay Kit (Pierce Biotechnology, Waltham, MA) following the

manufacturer's instructions. Light absorbance of these samples was measured at 595 nm on a Spectra MAX 190 spectrophotometer (Molecular Devices, Sunnyvale, CA). Total protein synthesized was determined from a standard curve of absorbance versus known concentrations of albumin run in parallel with experimental samples.

Alkaline phosphatase activity

Alkaline phosphatase activity in the cell lysates was determined by an Alkaline Phosphatase Assay Kit (Upstate, EMD Millipore, Billerica, MA, USA). Briefly, aliquots of the cell lysates were mixed with a 5 µL $NiCl_2$, 5 µL BSA, and 5 µL of a phosphopeptide solution in the wells of a microplate and the reaction mixture was incubated for 15 minutes at 37°C. Alkaline phosphatase activity was detected by adding 100 µL of a Green solution and measuring the absorbance of blank and standards at 650 nm using a spectrophotometer (Spectra MAX 190, Molecular Devices). Alkaline phosphatase activity was calculated by comparing absorbance values to a standard curve.

Cellular calcium deposition

The amount of calcium present in the acidic supernatant was then quantified using the Calcium Reagent Set by Pointe Scientific (Canton, MI) following the manufacturer's instructions. Absorbance of the samples was measured at 575 nm using a spectrophotometer (Spectra MAX 190, Molecular Devices). Total calcium was calculated from standard curves of absorbance versus known concentrations of calcium standards (Sigma-Aldrich) run in parallel with the experimental samples.

Statistical analysis

All experiments were conducted in triplicate at least three times. Data are expressed as the mean ± standard deviation (SD). Statistical significance was assessed by the two-tailed Student's *t*-test. A *P*-value <0.05 was considered to be statistically significant.

Results

Gel characterization: gelation, viscoelasticity and SEM

Gelation for gellan xanthan gels was tested by the inverted tube test for all three concentrations of gels: 0.9%, 0.7%, and 0.5% 9:1 gellan:xanthan in DMEM media. The gelation process was initialized immediately as the gel was allowed to cool down, for all three gel combinations. The storage and loss modulus for GX gels in DMEM media was also evaluated to check for gelation changes in the presence of ions in DMEM media. The storage vs loss modulus for gellan xanthan gels in DMEM showed a higher elastic modulus than the viscous moduli at lower frequency ranges (Figure 1A). Among the 3 concentrations tested, 0.9% 9:1 gellan xanthan showed the highest elastic modulus which indicates a mechanically strong gel as compared to the 0.7% and 0.5% gel combinations. The gels demonstrated a tendency of crossing over of the two moduli at higher frequency ranges. The combination (GX gels) showed a shear thinning effect at different shear stress for all concentrations tested which indicates ease of injectability of hydrogel (Figure 1B). The shear forces at the needle-tissue interface allow the gel to shear-thin and flow into the defect site. Upon removal of the shear stress, the polymer solution restores back its gel state indicating that the hydrogel could be delivered via an injection. The temperature of gelation was confirmed by viscosity vs temperature measurements. The gelation temperature for all three GX concentrations was found to be between 37°C–40°C, with the initiation of gelation at around 42°C (Figure 1C). However, not compromising on the gel strength as indicated in the frequency vs elastic and viscous modulus studies, 0.9% 9:1 gellan xanthan was utilized for further studies and for osteoblast differentiation studies.

Freeze dried hydrogel samples were examined by SEM studies at an accelerating voltage of 5 kV and 10 kV. The micrographs of the hydrogels showed a uniform cross-linked structure (Figure 2A and B), a property important for the mechanical strength as well as the water holding capacity of the gels.

Nanoparticle characterization

Particle size, zeta potential, TEM, and AFM

Particle size and polydispersity of the chitosan nanoparticles were determined by photon correlation spectroscopy which provides the hydrodynamic diameter of any colloidal particle. Chitosan nanoparticles with 0.2% chitosan and 0.2% TPP exhibited a hydrodynamic diameter of 297 ± 61 nm with a polydispersity index of 0.34. A zeta potential of +31.9 ± 2 mV was observed. The positive zeta potential of chitosan nanoparticles is a result of the residual amino groups. The higher the zeta potential, the more stable the particles are electro-kinetically. Chitosan nanoparticles with 0.2% TPP were monodispersed and had a smooth morphology with a particle size of around 200–300 nm with no aggregation as observed by TEM (Figure 3).

After the qualitative visualization of nanoparticles with TEM, the particle size and morphology were further confirmed quantitatively by AFM measurements

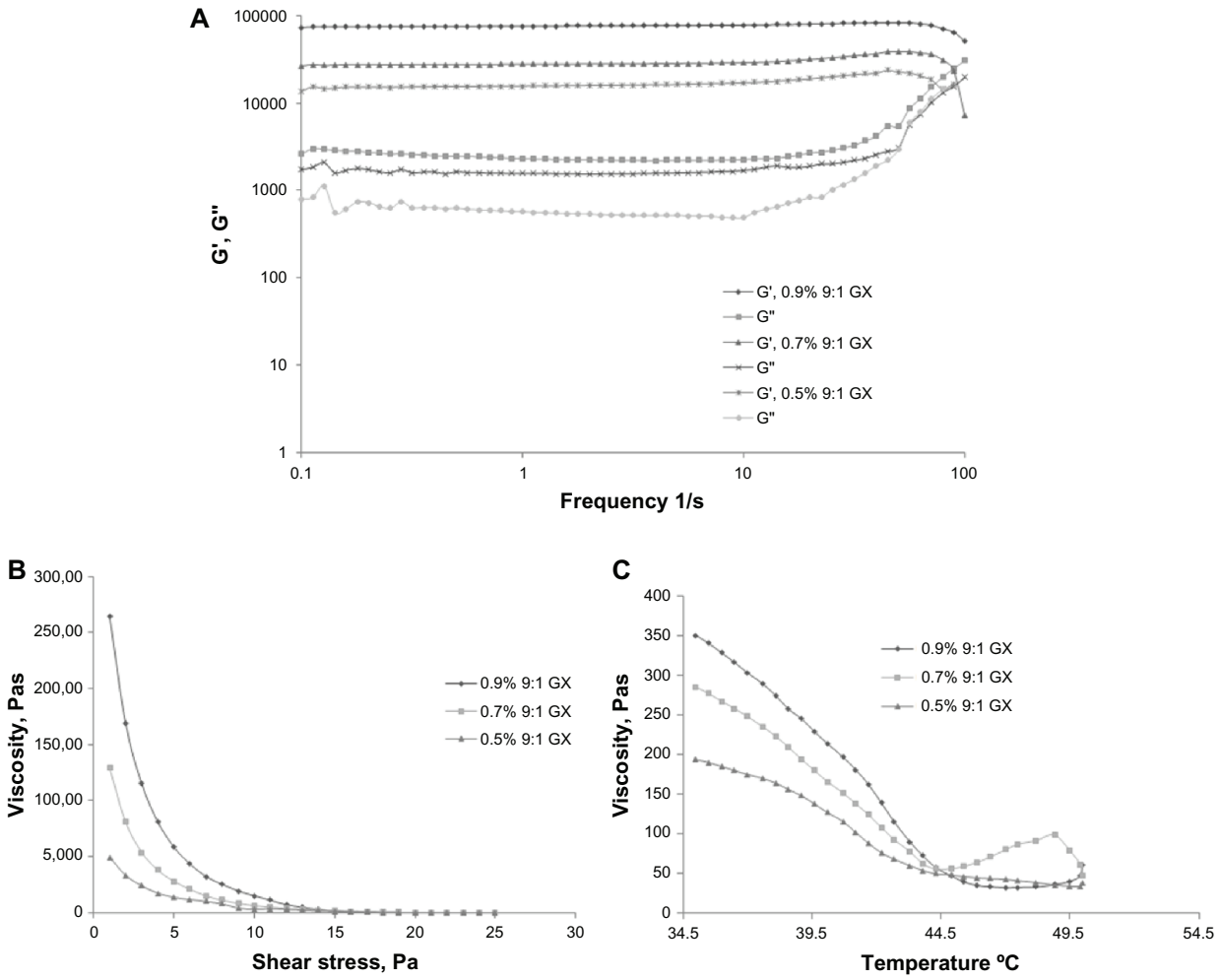

Figure 1 (**A**) Storage vs loss modulus of 0.9%, 0.7%, and 0.5% 9:1 gellan:xanthan gels. 0.9% gellan xanthan gels in DMEM showed a higher elastic modulus. (**B**) Viscosity vs shear stress and (**C**) viscosity vs temperature of three different combinations of gellan xanthan gels in DMEM.
Notes: Gelation process started at 42°C and the gelling temperature ranged between 37°C–40°C. Shear thinning effect observed.
Abbreviations: DMEM, Dulbecco's modified Eagle's medium; GX, gellan:xanthan; G′, Storage modulus; G″, Loss modulus; Pa Pascal.

in tapping mode. The particle size was found to be 214.84 ± 19.53 nm by AFM studies which were in agreement with the dynamic light scattering data obtained (Figure 4).

In vitro release

BMP7 was used as the osteogenic factor for human fetal osteoblast differentiation within gellan xanthan hydrogels.

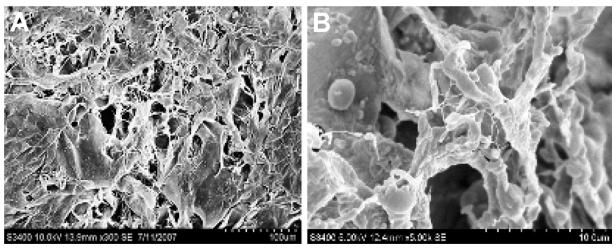

Figure 2 SEM of gellan xanthan gels showing the crosslinked structure. Accelerating voltage 5 kV (**A**) and 10 kV (**B**).
Abbreviation: SEM, scanning electron microscopy.

For BMP7 within hydrogels, an 80% release was observed by day 17 without a large initial burst release (Figure 5). After an initial burst release of about 10%, BMP7 entrapped in nanoparticles within hydrogels showed a cumulative release of 27% by day 17. BMP7 within hydrogels showed a cumulative release of 117.2 ng by day 6, whereas by day 11 and day 17 was found to be 192.7 and 275.5 ng, respectively, which was 82% of the BMP loaded initially. BMP in nanoparticles within gels showed 246 ng of growth factor release by day 11 whereas by day 17, 265 ng of drug had released which was 27% of the initial amount of BMP loaded (Figure 5).

Anti-bacterial properties

Chitosan nanoparticles demonstrated antibacterial activity with increasing concentration. Five milligrams per milliliter showed a higher anti-bacterial activity as compared to

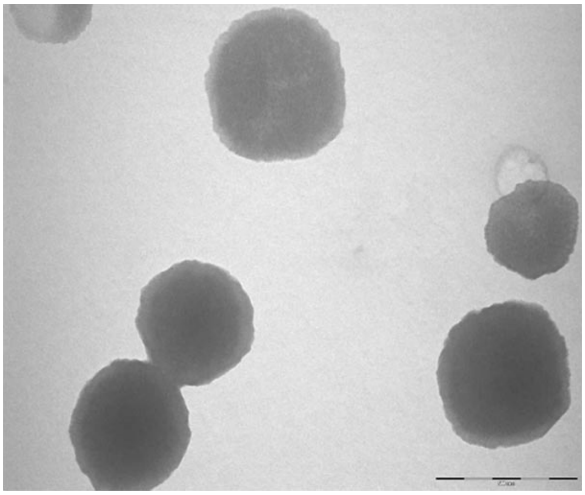

Figure 3 TEM of chitosan nanoparticles.
Note: Scale bar 500 nm.
Abbreviation: TEM, transmission electron microscopy.

2.5 mg/mL (Figure 6A). Gellan:xanthan gels used in the differentiation study, ie, 0.9% 9:1 gellan xanthan, were tested for antibacterial activity for the three different bacterial strains. The nanoparticle concentration within the gel was 1 mg/mL. No significant activity was seen in the case of *S. aureus* for all the gellan xanthan combinations (Figure 6B). All the combinations of gellan xanthan and nanoparticles showed excellent anti-bacterial activities for *P. aeruginosa* and *S. epidermidis* (Figure 6B).

In vitro toxicity: MTT assay and fluorescence imaging

Greater than 95% of L929 cells were viable in the presence of gellan xanthan gels. Osteoblast viability in presence of gellan xanthan gel components was found to be >80% as tested by the MTT assay at 48 hours.

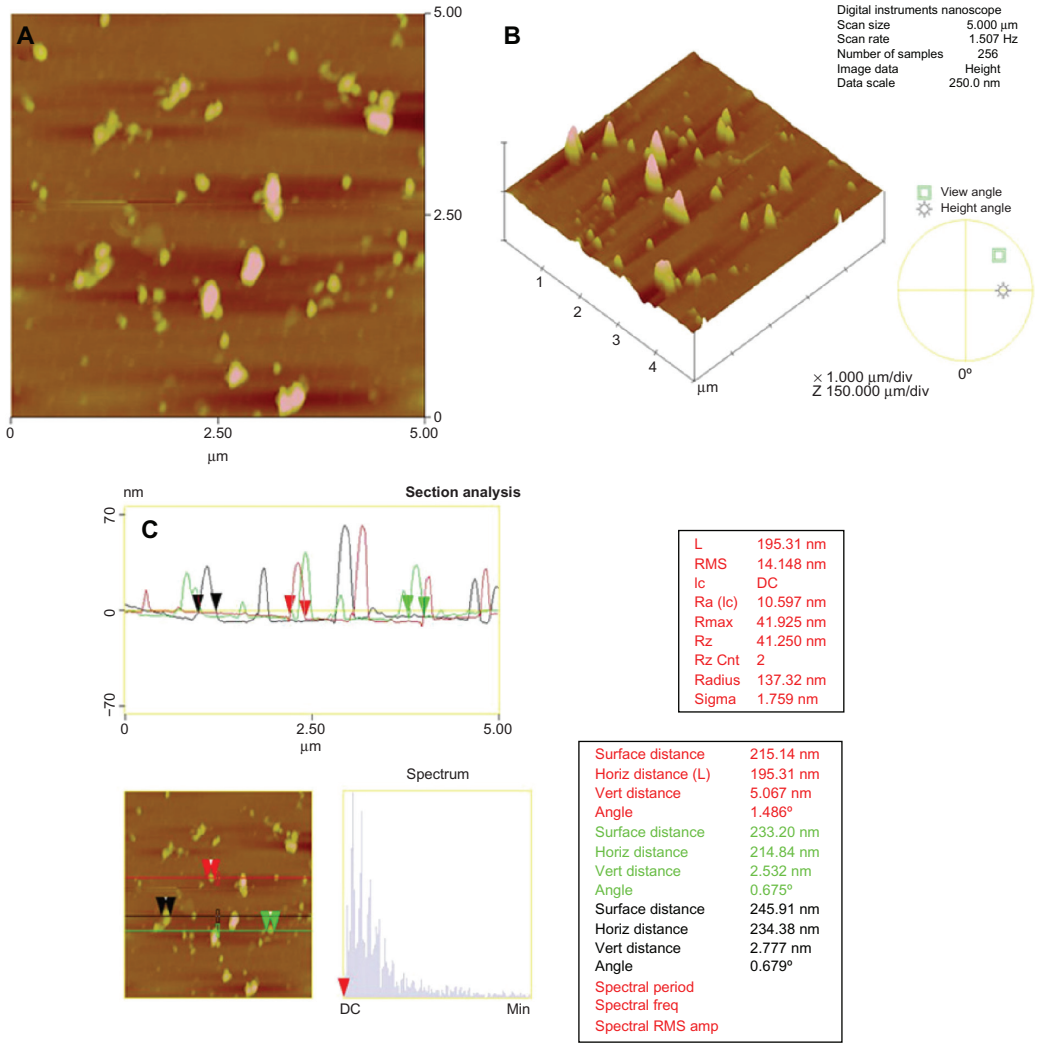

Figure 4 AFM micrographs and section analysis for chitosan nanoparticles.
Note: The particle size was found to be between 200–230 nm, as also observed in DLS. **A**, 2D image; **B**, 3D image; **C**, section analysis.
Abbreviations: AFM, atomic force microscopy; DC, direct current; DLS, dynamic light scattering.

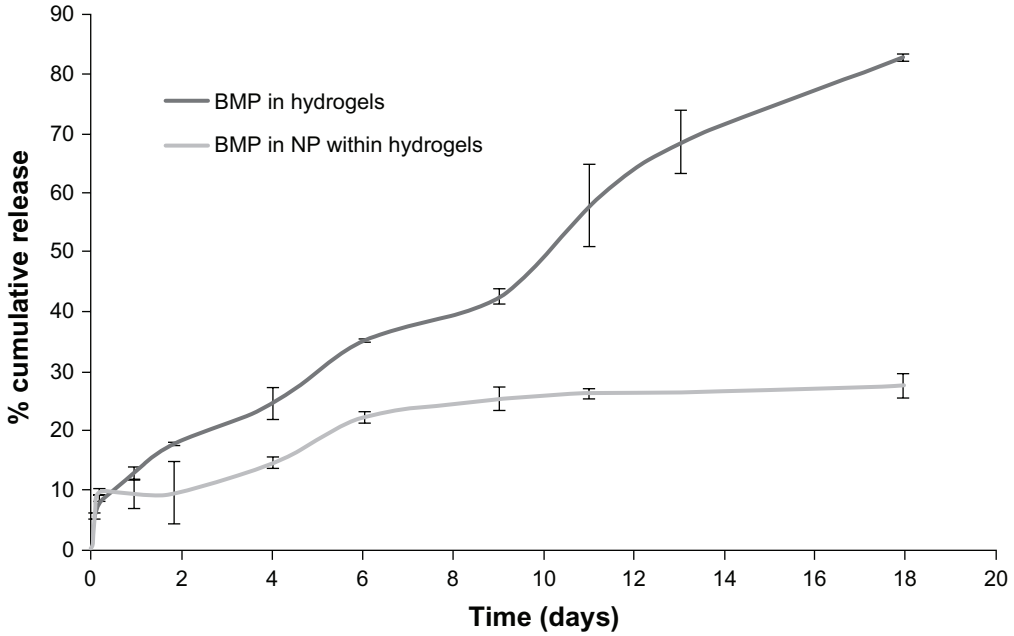

Figure 5 In vitro release of BMP7 from gellan xanthan gels and BMP7 from chitosan nanoparticles within gellan xanthan gels.
Abbreviations: BMP, bone morphogenetic protein; NP, nanoparticles.

Cells grown in the presence of the hydrogel extract exhibited a normal morphology as observed by confocal microscopy. DAPI stained the nucleus blue while the actin filaments were seen as red filamentous structures with rhodamine-phalloidin in the dual-dye staining of cells (Figure 7). Live/dead staining stained live cells as green (Calcein AM) and dead cells red (Ethidium homodimer, EthH). Osteoblasts were found to be viable within hydrogels suggesting that the environment could sustain osteoblast growth and proliferation (Figure 8A, B, and D). A very small percentage of dying cell population was observed by 48 hours with EthH staining (Figure 8C). The fluorescence studies indicated that cells maintained their morphology in the presence of the hydrogel samples and were viable by 48 hours. A Z scan of the hydrogels was conducted to assess the distribution of osteoblasts within the hydrogel matrix. The scan showed green fluorescence at the end of the 48 hour culture period at various scan depths indicating viable cells (Figure 9). The Z scan showed a greater number of viable cells within the 3D matrix of hydrogel which indicated that the hydrogel supported cell growth within its mesh like structure.

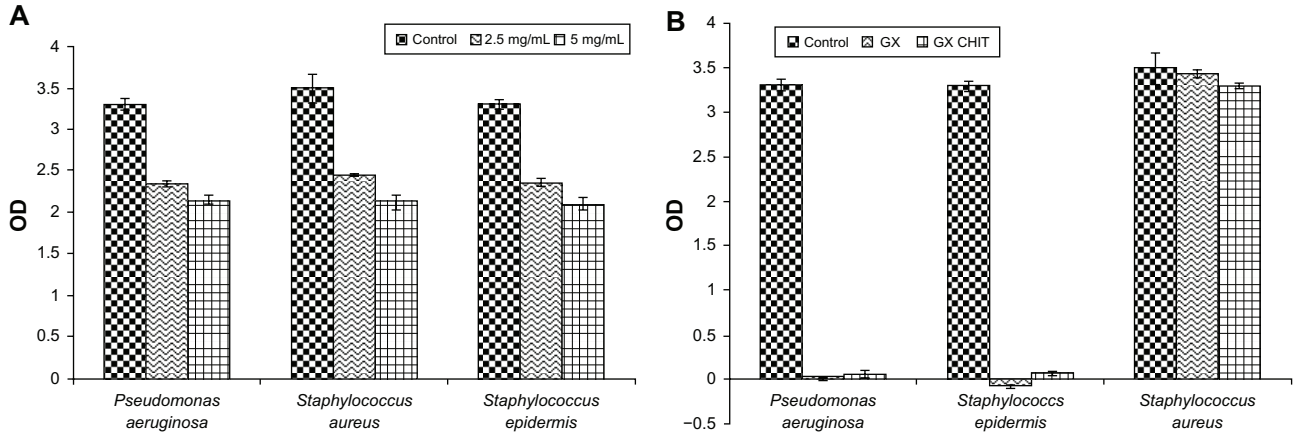

Figure 6 Antibacterial activity compared for 3 strains of bacteria for (**A**) chitosan, 2.5 and 1.25 mg/mL concentrations; (**B**) hydrogel components for *S. aureus*, *S. epidermidis*, and *P. aeruginosa*.
Abbreviations: GX, gellan:xanthan; CHIT, chitosan; OD, optical density.

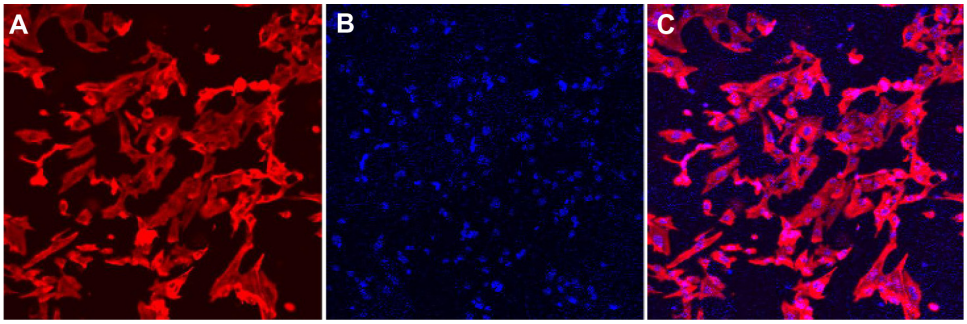

Figure 7 Rhodamine-phalloidin and DAPI stained osteoblast cells grown in gellan xanthan gels at 48 hours, (**A**) rhodamine phalloidin stained F-actin, (**B**) DAPI stained nuclei of osteoblasts, (**C**) merged image.
Abbreviation: DAPI, 4′,6-diamidino-2-phenylindole.

Osteoblast differentiation

Effect of different growth factors

Growth factor loaded gels vs the gellan xanthan control showed significant osteogenic differentiation. Growth factors such as BMP7 and bFGF have been shown to induce osteogenic differentiation in a time and dose-dependent manner in osteoblast cells with increased expression of alkaline phosphatase and calcium deposition as differentiation markers.[17–20] The effect of growth factors vs control gels showed higher differentiation markers in growth factor loaded gels. BMP7 demonstrated a higher total protein as compared to bFGF loaded gels (Figure 10A). On analyzing the effect of BMP7 vs bFGF, BMP7 showed significantly higher alkaline phosphatase (day 14, $P < 0.05$, Figure 10B) and calcium deposition (day 28, $P < 0.05$, Figure 10C), indicating a role in differentiation. Alkaline phosphatase for BMP7 by day 14 was observed to be 23 nanomoles per g of construct, while it was 17 nanomoles per g of construct for bFGF loaded gels. The values obtained were significantly higher than the control gel. It was observed that bFGF loaded gels had little role to play in osteoblast differentiation as seen by alkaline phosphatase synthesis by day 14, the values of which were comparable to control gels (Figure 10B). However, calcium deposition in bFGF was found to be higher than the control, but lower than BMP7 loaded gels (Figure 10C).

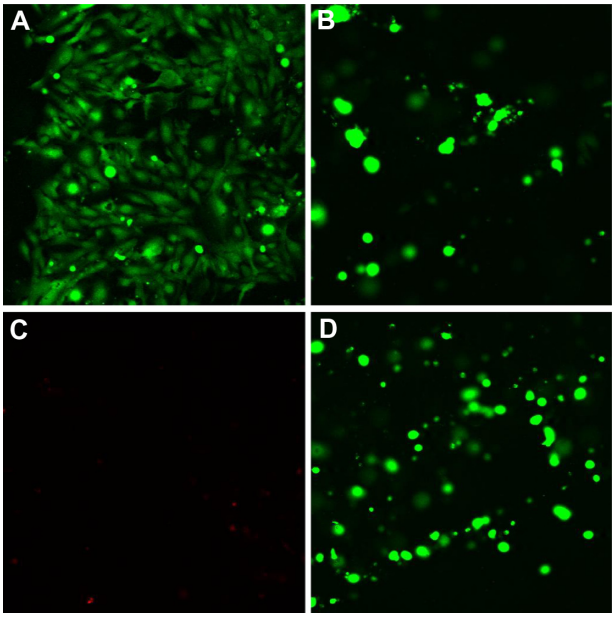

Figure 8 Live/dead staining using calcein AM and ethidium homodimer I of osteoblast grown within gellan xanthan gels after 48 hours, (**A**) gel extract, (**B**) live cells within the gel, (**C**) dead cells within the gel, (**D**) merged image (**B** and **C**).

Effect of single vs dual growth factors

Dual growth factor loaded gels showed a higher ability to promote osteoblast differentiation as compared to a single growth factor as observed in DNA content, alkaline phosphatase synthesis, and calcium deposition studies with significant differences observed at day 14 (Figure 11B, $P < 0.05$) and 28 (Figure 11C, $P < 0.05$). Figure 11 also demonstrates the effect of carrier entrapment: free vs entrapped growth factor on cell function. Nanoparticle entrapment of the growth factors showed a slow release profile and hence a significant increase in differentiation marker deposition by day 14 and 28. Day 3 values were found to have no significant differences between growth factor loaded and control gels which indicated an initial slow diffusion of bioactive growth factor to influence cell function.

It was observed that growth factor entrapment within nanoparticles showed a prolonged sustained growth factor release and hence a significantly different calcium content visible at day 28 (Figure 11C). Day 3 values for calcium deposition and alkaline phosphatase activity were found to be non-significant in all the groups tested: control gels,

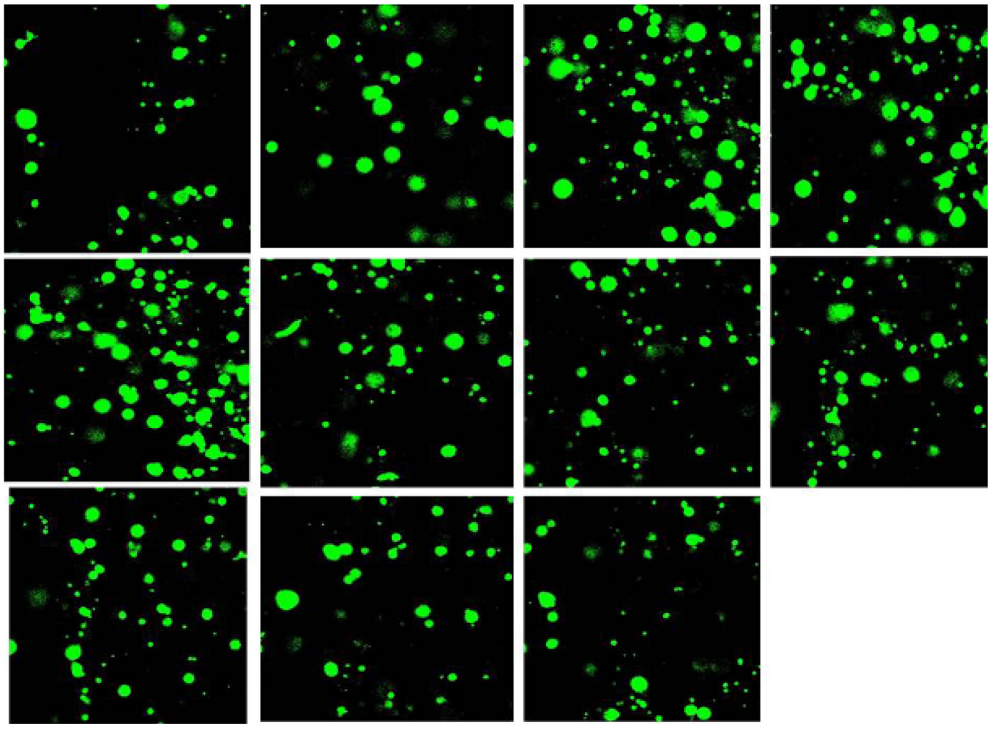

Figure 9 Z scan of osteoblast cultured within gellan xanthan gels at a scan depth of 200 microns.

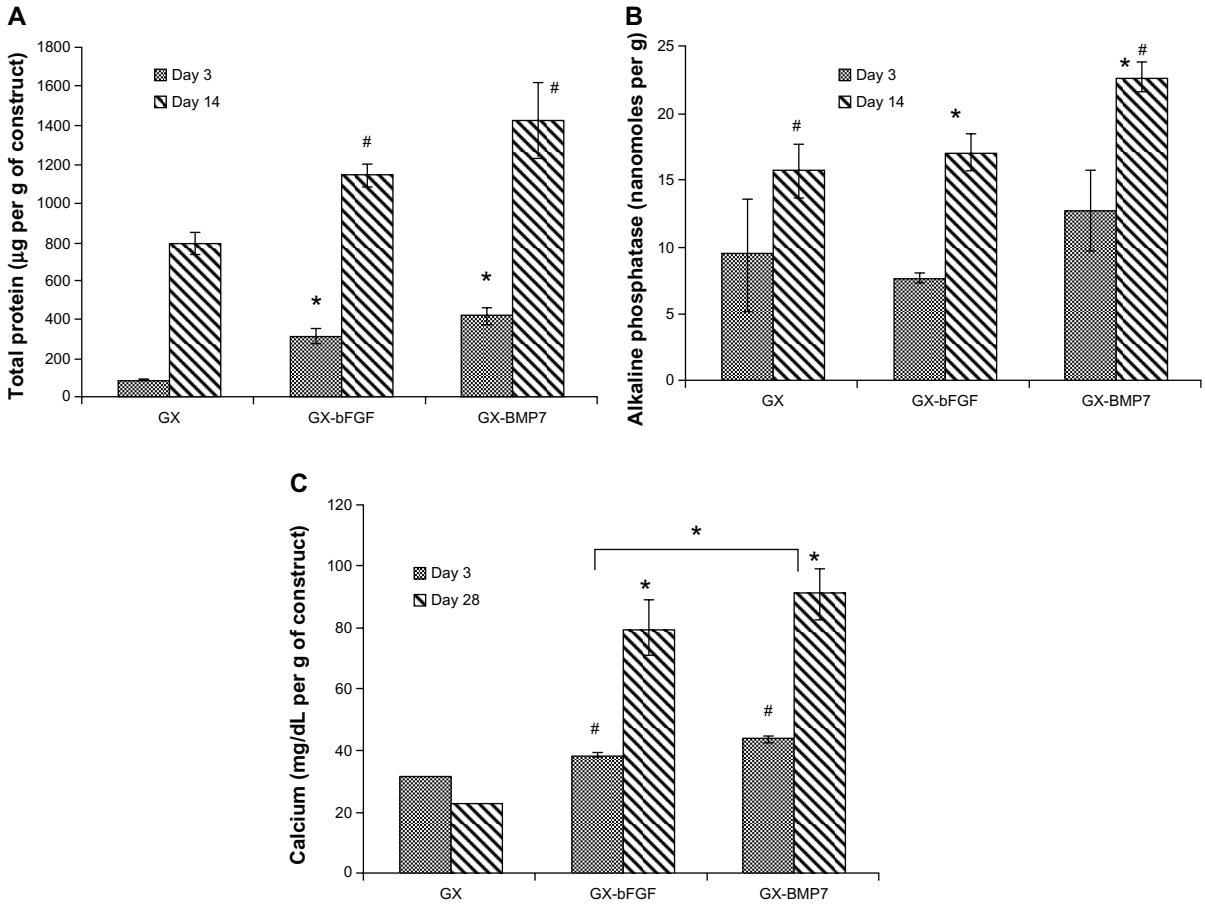

Figure 10 Effect of different growth factors on (**A**) total protein (**B**) alkaline phosphatase (**C**) calcium content.
Notes: #*P* < 0.05 as compared to controls and within groups.
Abbreviations: GX, gellan:xanthan; bFGF, basic fibroblast growth factor; BMP, bone morphogenetic protein.

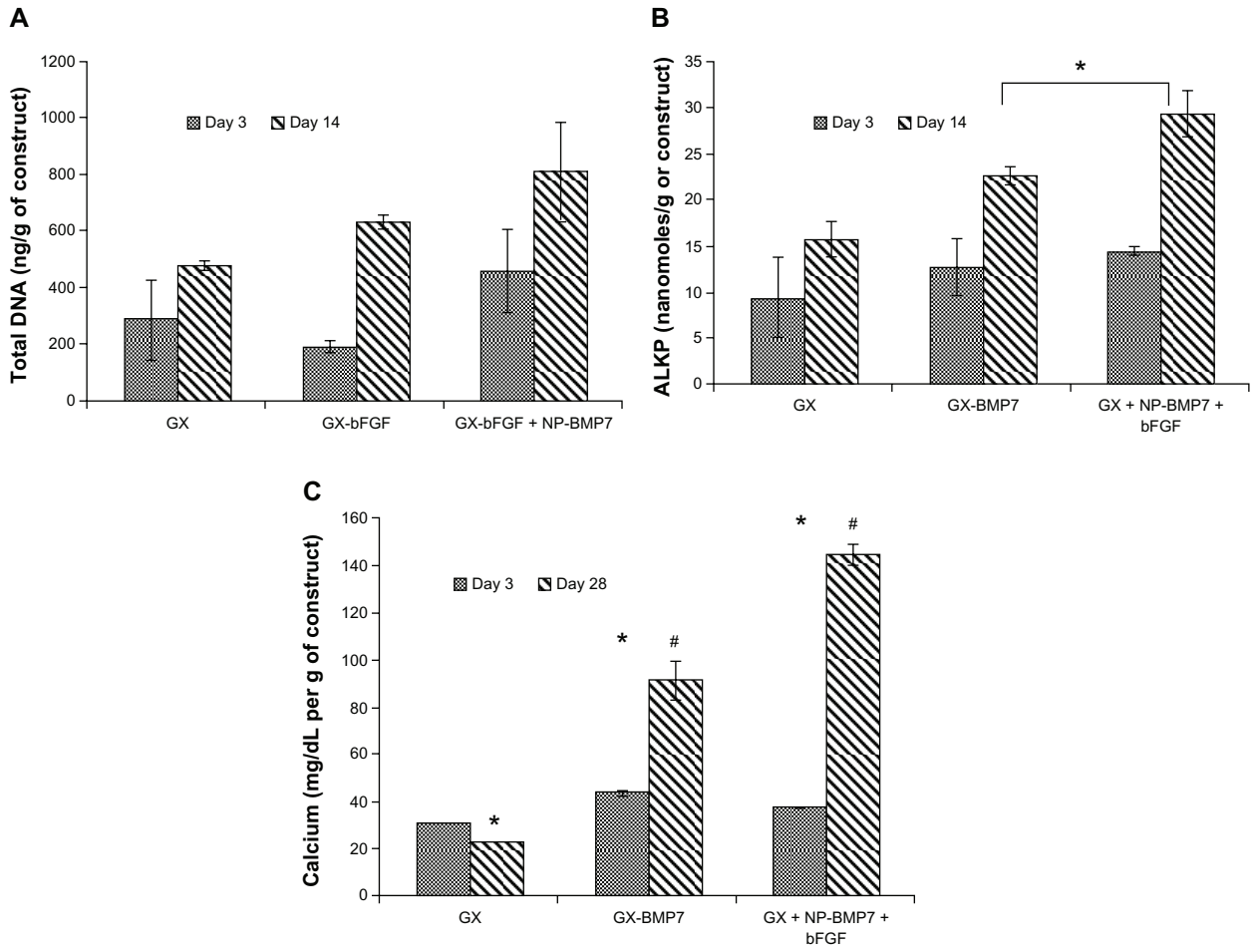

Figure 11 Effect of single vs dual growth factor (**A**) total DNA (**B**) alkaline phosphatase (**C**) calcium content.
Notes: #*$P < 0.05$ as compared to control and within groups.
Abbreviations: GX, gellan:xanthan; bFGF, basic fibroblast growth factor; BMP, bone morphogenetic protein; NP, chitosan nanoparticles.

free growth factor, and dual entrapped growth factor, which could be due to the slow manifestation of the effects of the small amount of growth factor release due to different barriers to growth factor release.

Discussion

An injectable dual growth factor loaded hydrogel system for bone tissue engineering applications was developed and evaluated for osteoblast differentiation. The hydrogels showed a porous network structure that ensured a suitable microenvironment for osteoblast proliferation. bFGF release has been reported in earlier studies by our group.[11] bFGF within chitosan nanoparticles showed a cumulative release percentage of 80% by day 20. bFGF encapsulated within hydrogel-entrapped chitosan nanoparticles had a further slower release with a cumulative percentage release of around 49% by day 21.[30] The initial burst in the release profile was observed due to the soaking method used for growth factor entrapment within nanoparticles which caused the growth factor on the surface of nanoparticles to elute out first. Entrapment of growth factors within nanoparticles allowed a controlled release of the growth factor meeting the temporal requirement of the protein at each stage of differentiation. The release properties could be modified by the choice of growth factors to be entrapped within the hydrogel matrix and nanoparticles.

The advantage of dual growth factor loading was clearly observed with an increase in the marker amounts as evaluated with different marker assays. The effect of multiple growth factors on chondrogenesis and osteogenesis in mesenchymal stem cells (MSCs) has been reported.[31,32] Studies reporting dual growth factor delivery (delivery of TGF-β and BMP7) in alginate gels[33] and polycaprolactone/pluronic F127 porous scaffolds[34] have shown sequential growth factor release. However, the effect of encapsulation of the two growth factors within a carrier system on differentiation has not been reported yet. Also, none of the studies report an injectable system with dual growth factor delivery.

Our group has demonstrated MSC differentiation in the presence of platelet derived growth factor-bb and bFGF loaded chitosan nanoparticles within gellan xanthan gels for cartilage regeneration.[11] The current study was an attempt to evaluate a similar system with osteoblast cells as a potential dual growth factor delivering bone tissue engineering construct. The study showed a high alkaline phosphatase activity and mineralization in the growth factor loaded gels as compared to controls. Chitosan has been shown to upregulate several genes associated with mineralization.[35] The increased mineralization observed in the calcium deposition study can be attributed to a combinatorial effect of chitosan nanoparticles and BMP7.

The novelty of the construct is its injectability and ease of administration via an injection, eliminating the need for surgery to place the implant into the body. Such an injectable system with dual growth factors allowing bone cells to differentiate has not been reported yet. For achieving mechanical strengths similar to that of cancellous bone, calcium phosphate nanotubes or nanohydroxyapatite crystals may be incorporated within the hydrogel system. Chandanshive et al[28] report synthesis and characterization of calcium phosphate nanotubes that have shown excellent biocompatibility and cellular uptake. Internalization of nanotubes within L929 cells have proven the biomaterial to be an effective carrier system that could be incorporated into the hydrogel system for growth factor delivery.[28]

To conclude, the nanoparticulate gellan xanthan gel incorporating chitosan nanoparticles serves as a platform technology which is a minimally invasive, injectable scaffold with appropriate growth factor delivery over weeks to facilitate cellular differentiation.

Acknowledgments

The authors would like to acknowledge the Indo-US Joint Centre on Biomaterials for Healthcare funded by the Indo-US Science and Technology Forum (IUUSTF), New Delhi, India, for providing funds for travel and work; and Dr Yupeng Chen and Dr Bahar Bilgen from Brown University, Providence, Rhode Island, USA for providing their valuable input in the research. The authors would also like to acknowledge Centre for Research in Nanotechnology and Science (CRNTS), Industrial Research and Consultancy Centre (IRCC), and Indian Institute of Technology Bombay (IIT Bombay) for providing instrument facilities for material characterization.

Disclosure

The authors report no conflicts of interest in this work.

References

1. Zhang L, Rodriguez J, Raez J, Myles AJ, Fenniri H, Webster TJ. Biologically inspired rosette nanotubes and nanocrystalline hydroxyapatite hydrogel nanocomposites as improved bone substitutes. *Nanotechnology*. 2009;20(17):175101.
2. Weinand C, Pomerantseva I, Neville CM, et al. Hydrogel-β-TCP scaffolds and stem cells for tissue engineering bone. *Bone*. 2006;38(4):555–563.
3. Burdick JA, Mason MN, Hinman AD, Thorne K, Anseth KS. Delivery of osteoinductive growth factors from degradable PEG hydrogels influences osteoblast differentiation and mineralization. *J Control Release*. 2002;83:53–63.
4. Balasundaram G, Webster TJ. An Overview of Nano-Polymers for Orthopedic Applications. *Macromol Biosci*. 2007;7(5):635–642.
5. Bokhari MA, Akay G, Zhang S, Birch MA. The enhancement of osteoblast growth and differentiation in vitro on a peptide hydrogel–polyHIPE polymer hybrid material. *Biomaterials*. 2005;26(25):5198–5208.
6. Grasdalen H, Smidsrød O. Gelation of Gellan Gum. *Carbohydr Polym*. 1987;7(5):371–393.
7. Sutherland IW. Novel and established applications of microbial polysaccharides. *Trends Biotechnol*. 1998;16(1):41–46.
8. Oliveira JT, Martins L, Picciochi R, et al. Gellan gum: A new biomaterial for cartilage tissue engineering applications. *J Biomed Mater Res A*. 2010;93(3):852–863.
9. Oliveira JT, Santos TC, Martins L, et al. Gellan gum injectable hydrogels for cartilage tissue engineering applications: In vitro studies and preliminary in vivo evaluation. *Tissue Eng Part A*. 2010;16(1):343–353.
10. Oliveira JT, Gardel LS, Rada T, Martins L, Gomes ME, Reis RL. Injectable gellan gum hydrogels with autologous cells for the treatment of rabbit articular cartilage defects. *J Orthop Res*. 2010;28(9):1193–1199.
11. Dyondi D, Chandra V, Bhonde RR, Banerjee R. Development and characterization of dual growth factor loaded in situ gelling biopolymeric system for tissue engineering applications. *J Biomater Tissue Eng*. 2012;2(1):67–75.
12. Babensee JE, McIntire LV, Mikos AG. Growth factor delivery for tissue engineering. *Pharm Res*. 2000;17(5):497–504.
13. Heckman JD, Boyan BD, Aufdemorte TB, Abbott JT. The use of bone morphogenetic protein in the treatment of non-union in a canine model. *J Bone Joint Surg Am*. 1991;73(5):750–764.
14. Laflamme C, Curt S, Rouabhia M. Epidermal growth factor and bone morphogenetic proteins upregulate osteoblast proliferation and osteoblastic markers and inhibit bone nodule formation. *Arch Oral Biol*. 2010;55(9):689–701.
15. Mundy GR. Regulation of bone formation by bone morphogenetic proteins and other growth factors. *Clin Orthop Relat Res*. 1996;324:24–28.
16. Sampath TK, Maliakal JC, Hauschka PV, et al. Recombinant human osteogenic protein (hOP-1) induces new bone formation in vivo with specific activity comparable to natural bovine osteogenic protein and stimulates osteoblast proliferation and differentiation in vitro. *J Biol Chem*. 1992;267(28):20352–20362.
17. Knutsen R, Wergedal JE, Sampath TK, Baylink DJ, Mohan S. Osteogenic protein-1 stimulates proliferation and differentiation of human bone cells in vitro. *Biochem Biophys Res Commun*. 1993;194(3):1352–1358.
18. Cheng H, Jiang W, Phillips FM, et al. Osteogenic activity of the fourteen types of human bone morphogenetic proteins (BMPs). *J Bone Joint Surg Am*. 2003;85-A(8):1544–1552.
19. Canalis E, Lian JB. Effects of bone associated growth factors on DNA, collagen and osteocalcin synthesis in cultured fetal rat calvariae. *Bone*. 1988;9(4):243–246.
20. Hosokawa R, Kikuzaki K, Kimoto T, et al. Controlled local application of basic fibroblast growth factor (FGF-2) accelerates the healing of GBR. An experimental study in beagle dogs. *Clin Oral Implants Res*. 2000;11(4):345–353.
21. Tabata Y, Yamada K, Miyamoto S, et al. Bone regeneration by basic fibroblast growth factor complexed with biodegradable hydrogels. *Biomaterials*. 1998;19(7–9):807–815.

22. Li P, Poon YF, Li W, et al. A polycationic antimicrobial and biocompatible hydrogel with microbe membrane suctioning ability. *Nat Mater*. 2011;10(2):149–156.
23. Campoccia D, Montanaro L, Arciola CR. The significance of infection related to orthopedic devices and issues of antibiotic resistance. *Biomaterials*. 2006;27(11):2331–2339.
24. Calvo P, Remuñán-López C, Vila-Jato JL, Alonso MJ. Novel hydrophilic chitosan-polyethylene oxide nanoparticles as protein carriers. *J Appl Polym Sci*. 1997;63(1):125–132.
25. Schierlohz JM, Beuth J. Implant infections: a haven for opportunistic bacteria. *J Hosp Infect*. 2001;49(2):87–93.
26. Puckett SD, Taylor E, Raimondo T, Webster TJ. The relationship between the nanostructure of titanium surfaces and bacterial attachment. *Biomaterials*. 2010;31(4):706–713.
27. Tran N, Mir A, Mallik D, Sinha A, Nayar S, Webster TJ. Bactericidal effect of iron oxide nanoparticles on Staphylococcus aureus. *Int J Nanomedicine*. 2010;5:277–283.
28. Chandanshive B, Dyondi D, Ajgaonkar VR, Banerjee R, Khushalani D. Biocompatible calcium phosphate based tubes. *J Mater Chem*. 2010;20:6923–6928.
29. Chen Y, Webster TJ. Increased osteoblast functions in the presence of BMP-7 short peptides for nanostructured biomaterial applications. *J Biomed Mater Res A*. 2008;91(1):296–304.
30. Dyondi D, Webster TJ, Banerjee R. Development of a dual growth factor loaded biodegradable hydrogel and its evaluation on osteoblast differentiation in vitro. *MRS Proceedings*. 2011;1312.
31. Kim HJ, Im GI. Combination of transforming growth factor-beta2 (TGFβ2) and bone morphogenetic protein 7 (BMP7) enhances chondrogenesis from adipose tissue-derived mesenchymal stem cells. *Tissue Eng Part A*. 2009;15(7):1543–1551.
32. Park JS, Yang HN, Woo DG, Jeon SY, Park KH. The promotion of chondrogenesis, osteogenesis, and adipogenesis of human mesenchymal stem cells by multiple growth factors incorporated into nanosphere-coated microspheres. *Biomaterials*. 2011;32(1):28–38.
33. Lim SM, Oh SH, Lee HH, Yuk SH, Im GI, Lee JH. Dual growth factor-releasing nanoparticle/hydrogel system for cartilage tissue engineering. *J Mater Sci Mater Med*. 2010;21(9):2593–2600.
34. Lim SM, Jang SH, Oh SH, Yuk SH, Im GI, Lee JH. Dual-growth-factor-releasing PCL scaffolds for chondrogenesis of adipose-tissue-derived mesenchymal stem cells. *Adv Eng Mater*. 2010;12:62–69.
35. Mathews S, Gupta PK, Bhonde R, Totey S. Chitosan enhances mineralization during osteoblast differentiation of human bone marrow-derived mesenchymal stem cells, by upregulating the associated genes. *Cell Prolif*. 2011;44(6):537–549.